

AD-A125 609

OPTICAL SIGNAL PROCESSING(U) DYNAMIC SYSTEMS INC MCLEAN 1/1  
VA 14 FEB 83 N00014-81-C-2560

UNCLASSIFIED

F/G 9/4

NL

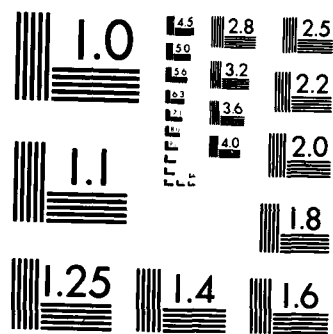


END

FILMED

JPL

DTIC



MICROCOPY RESOLUTION TEST CHART  
NATIONAL BUREAU OF STANDARDS-1963-A

12

AD A 1 256 034

FINAL REPORT

OPTICAL SIGNAL PROCESSING

N00014-81-C-2560

14 February 1983

Prepared by

Dynamic Systems, Inc.  
8200 Greensboro Drive, Suite 500  
McLean, Virginia 22102

MAR 14 1983

A

This document has been approved  
for public release and sale; its  
distribution is unlimited.

OTIC FILE COPY

88 02 023 087

## TABLE OF CONTENTS

	<u>Page</u>
1.0 INTRODUCTION.....	1-1
2.0 RESULTS.....	2-1
2.1 Multiplexed Coherent Optical Processor.....	2-1
2.2 Application of Outer Product Operation to Matrix-Matrix Multiplication.....	2-1
2.3 Optical and Digital Techniques for Performing Hankel Transforms.....	2-2




✓  
*Added on file*

A

## 1.0 INTRODUCTION

Optical signal processing makes possible rapid coordinate transformations, optical pattern recognition, and matrix-matrix multiplication. In the present contract, DSI has demonstrated several significant accomplishments. Among these are: (a) the design and operation of a spatial-frequency-multiplexed coherent optical processor; (b) the application of outer product operation to matrix-matrix multiplication; and (c) the description of three methods for performing Hankel transforms with optical or digital processors.



## 2.0 RESULTS

The accomplishments described below are important in a number of areas. The optical information processing projects described have application to mode analysis of high energy laser resonators, alignment of space telescopes, and tomographic reconstruction. The progress in coherent optical moment generation is of value in image data compression and optical pattern recognition of statistical images. Finally, the acoustooptic matrix signal processor constructed is useful in radar signal processing, passive sonar surveillance, and adaptive beam forming.

### 2.1 MULTIPLEXED COHERENT OPTICAL PROCESSOR

A coherent optical processor designed for calculating generalized moments of a two-dimensional pattern<sup>1</sup> is described in Enclosure (1). In order to provide for parallel computation of multiple moments, a spatial-frequency multiplexing scheme was used. A computer-generated holographic mask was shown to provide complete flexibility in choosing moment generated functions. The calculation of five geometric moments was experimentally demonstrated for simple objects. These geometric moments correspond to  $x$ ,  $y$ ,  $xy$ ,  $x^2$ , and  $y^2$ .

A computer-generated holographic mask was constructed to compute the geometric moments corresponding to the generating functions,  $x$ ,  $y$ ,  $xy$ ,  $x^2$ , and  $y^2$ . In order to reduce the dynamic range problems, when the hologram was constructed the scale of the generating functions was chosen such that the linear and quadratic-moment values would be equal for a symmetric object threefourths the linear size of the mask. The spacing chosen avoided crosstalk between adjacent moments. Since several generating functions are encoded on a single mask, the optical processor is able to calculate several moments in parallel.

### 2.2 APPLICATION OF OUTER PRODUCT OPERATION TO MATRIX-MATRIX MULTIPLICATION

The systolic architecture proposed by Caulfield and Rhodes<sup>2</sup> for matrix-matrix multiplication was utilized. This approach bypasses the two-dimensional

real time spatial light modulators required by other architectures. Various implementations of this optical processor<sup>3</sup> can use one of the following modulation mechanisms: (a) electrooptic, (b) direct driven LED array, and (c) acousto-optic (e.g., Bragg cells). These three approaches are described in Enclosure (2).

### 2.3 OPTICAL AND DIGITAL TECHNIQUES FOR PERFORMING HANKEL TRANSFORMS

Generalized Hankel transforms are useful in analyzing the effect of circularly symmetric optical systems on arbitrary inputs. Some examples of such systems are complex laser resonators and space telescopes. Three methods for performing Hankel transforms with optical or digital processors were described<sup>4</sup>. The first method was applicable when the input data is available in cartesian (x-y) format and used the close connection between generalized Hankel transform and the two-dimensional Fourier transform in cartesian coordinates. The second method was useful when the input data is in polar (r- $\theta$ ) format and used change of variables to perform the  $n^{\text{th}}$  order Hankel transform as a correlation integral. The third method utilized the von Neumann addition theorem for Bessel Functions to extract the Hankel coefficients from a correlation between the radial part of the input and a Bessel function. Initial experimental results<sup>4</sup> obtained for optical implementation of the first two methods are presented in Enclosure (3).

The analysis of complex optical systems is greatly facilitated by two-dimensional Fourier techniques. The effect of an optical system on arbitrary inputs is easily described by a transfer function in the Fourier domain. Generalized Hankel transform is similarly useful when dealing with a circularly symmetric (or axisymmetric) system for arbitrary inputs. This situation is encountered in performing mode analysis on the output of a slightly misaligned laser resonator as well as in aligning space telescopes. An optical method for performing mode analysis via generalized Hankel transform has the unique advantage of preserving the phase of the wavefront to be analyzed.

# REFERENCES

1. J. Blodgett, et.al., Opt. Lett. 7, 7 (1982)
2. H. Caulfield, et.al., Opt. Comm. 40, 86 (1981)
3. R. Athale and W. Collins, Appl. Opt. 21, 2089 (1982)
4. R. Athale, et.al., Opt. Lett. 7, 124 (1982)



# Multiplexed coherent optical processor for calculating generalized moments

J. A. Blodgett, R. A. Athale, C. L. Giles,\* and H. H. Szu

U.S. Naval Research Laboratory, Washington, D.C. 20375

Received September 28, 1981

A coherent optical processor capable of calculating generalized moments of a two-dimensional pattern is described. A spatial-frequency multiplexing scheme is used to provide for parallel computation of multiple moments. The use of a computer-generated holographic mask permits complete flexibility in choosing moment-generating functions; e.g., the functions could be complex or have a predetermined weighting function. Experimentally, calculation of five geometric moments (corresponding to  $x$ ,  $y$ ,  $xy$ ,  $x^2$ , and  $y^2$ ) is demonstrated for simple objects. The special features of the proposed coherent optical processor and its space-bandwidth requirements are also discussed.

The role of moments and moment invariants as global features in pattern recognition is well known.<sup>1-3</sup> Coherent optical processors for calculating geometric moments of images have been recently proposed,<sup>4,5</sup> but both of these processors are restricted to calculating geometric moments only. In addition, the processor of Ref. 4 is rather complicated, involving interferometric setups; the processor of Ref. 5 has an added factor  $1/(p!q!)$  associated with the  $pq$ th moment, further compounding the dynamic-range problems. In this Letter we propose a spatial-frequency-multiplexed coherent optical processor that overcomes these limitations. We describe the design and operation of this processor, present the initial experimental results obtained with it, and summarize its special features and limitations.

The generalized moment  $G_{mn}$  of a two-dimensional pattern  $f(x, y)$  is defined as

$$G_{mn} = \int_{-\infty}^{\infty} \int_{-\infty}^{\infty} f(x, y) g_{mn}(x, y) dx dy, \quad (1)$$

where  $g_{mn}(x, y)$  is the generating function. One way of calculating the inner product of Eq. (1) optically is to multiply the input  $f(x, y)$  by the generating function  $g_{mn}(x, y)$  and then take a two-dimensional Fourier transform of the product. The moment  $G_{mn}$  is obtained at the origin of the frequency plane:

$$G_{mn} = \int_{-\infty}^{\infty} \int_{-\infty}^{\infty} f(x, y) g_{mn}(x, y) \times \exp[-j(ux + vy)] dx dy \Big|_{\substack{u=0 \\ v=0}}. \quad (2)$$

If  $g_{mn}(x, y)$  is multiplied by a spatial carrier of the form  $\exp[j(mu_0x + nu_0y)]$ , then the desired moment is obtained at  $u = mu_0$ ,  $v = nu_0$  in the frequency plane

$$G_{mn} = \int_{-\infty}^{\infty} \int_{-\infty}^{\infty} f(x, y) g_{mn}(x, y) \exp[-j((u - mu_0)x + (v - nu_0)y)] dx dy \Big|_{\substack{u=mu_0 \\ v=nu_0}}. \quad (3)$$

Now if the function  $g(x, y)$ , which multiplies the input  $f(x, y)$ , has the form

$$g(x, y) = \sum_{m=-M}^M \sum_{n=-N}^N g_{mn}(x, y) \exp[j(mu_0x + nu_0y)], \quad (4)$$

then the output of the optical processor will contain the desired generalized moments  $G_{mn}$  ( $m = -M, \dots, 0, \dots, M$  and  $n = -N, \dots, 0, \dots, N$ ) provided that the unit carrier frequency ( $u_0, v_0$ ) satisfies the conditions discussed below. Figure 1 is a schematic diagram of the optical processor. It consists simply of a mask containing  $g(x, y)$  described by Eq. (4) and a Fourier-transform lens. A two-dimensional array of detectors measures the light intensity at discrete points in the Fourier plane, giving  $|G_{mn}|^2$ . Since the function  $g(x, y)$  is bipolar in the case of geometric moments and could be complex for some other choices of generating functions, it is necessary to make the mask holographically. In particular, a computer-generated hologram will provide maximum operational flexibility to the coherent optical processor.

To demonstrate the operation of the coherent optical processor described above, a computer-generated holographic mask was constructed to compute the geometric moments  $m_{10}$ ,  $m_{01}$ ,  $m_{11}$ ,  $m_{20}$ , and  $m_{02}$  (corresponding to generating functions  $x$ ,  $y$ ,  $xy$ ,  $x^2$ , and  $y^2$ , respectively). When the hologram was constructed the generating functions were scaled such that the linear- and quadratic-moment values would be equal for a

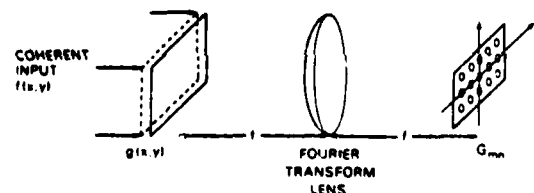


Fig. 1. Schematic diagram of a multiplexed coherent optical processor for calculating generalized moments.

ENCLOSURE (1)

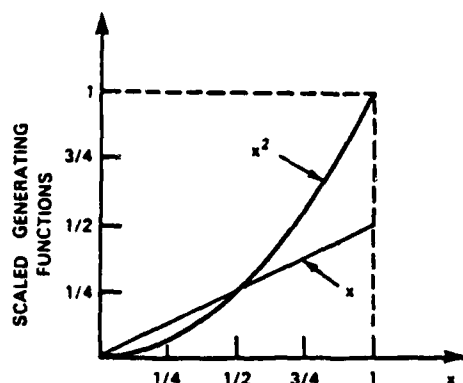


Fig. 2. Plot of the generating functions  $x$  and  $x^2$  with  $x$  multiplied by a weight of 0.5.

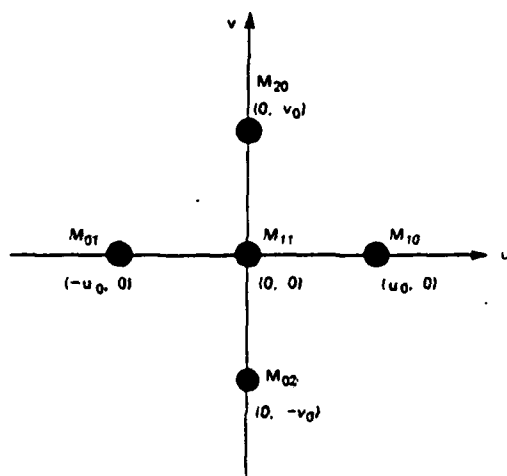


Fig. 3. Arrangement of the five geometric moments in the output plane.

symmetric object three fourths the linear size of the mask (Fig. 2). This was done to alleviate the dynamic-range problems in making the mask. The arrangement of the five moments in the output plane is shown in Fig. 3. The spacing was chosen to avoid cross talk between adjacent moments. It should be noted that the arrangement is determined by the spatial carrier multiplying the different generating functions and hence is completely under experimental control. The computer-generated holograms, which used the Lee-Burckhardt encoding scheme,<sup>6</sup> contained  $216 \times 216$  pixels and had physical dimensions of  $16.2 \text{ mm} \times 16.2 \text{ mm}$ . The output was detected by a video camera with a PbO target. The  $\gamma$  of the camera was adjusted to be  $\approx 1$ ; hence the electrical signal was proportional to the light intensity. The output of the camera was digitized and stored in a minicomputer for further analysis.

The coherent optical processor was used to calculate these five geometric moments for simple inputs. A photograph of the output for a binary square input image is displayed as Fig. 4. The moments are measured at the center of each of the five patterns. The  $m_{10}$  and  $m_{01}$  moments are seen to be zero, indicating that the input had symmetry about the  $Y$  and  $X$  axes, respectively. A line scan through the  $m_{10}$  pattern clearly

shows the null at the center, as depicted in Fig. 5(a). When the input was translated by  $\sim 10\%$  of its linear dimension along the  $X$  axis (thus removing the symmetry about the  $Y$  axis), a nonzero value for  $m_{10}$  is obtained, as is seen in Fig. 5(b).

The line scans through  $m_{20}$  and  $m_{02}$  moments of a binary rectangular input with a 2:1 aspect ratio and  $X$ - and  $Y$ -axis symmetry are displayed in Fig. 6. The theoretical value of the ratio  $|m_{20}/m_{02}|^2$  is 16, whereas the experimentally measured value is 16.3, corresponding to an error of  $\sim 1.9\%$ . A detector with better dynamic range and linearity should result in improved accuracy.

In this Letter we have described a coherent optical processor designed for calculating generalized moments of a two-dimensional pattern. A computer-generated hologram is used to encode several generating functions on one mask with spatial-frequency encoding. This special feature enables the processor to calculate several moments in parallel. The use of a computer-generated hologram makes it possible to encode complex generating functions and permits predetermined weighting functions to be used for dynamic-range consideration.

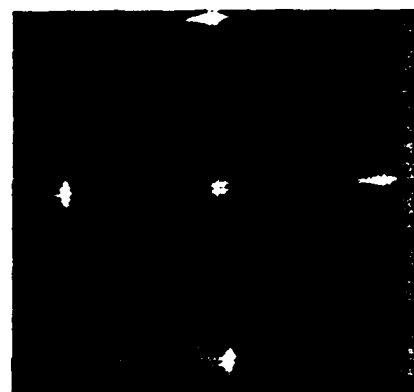


Fig. 4. Photograph of the output of the optical processor. The input was a square binary object with  $x$  and  $y$  symmetry.

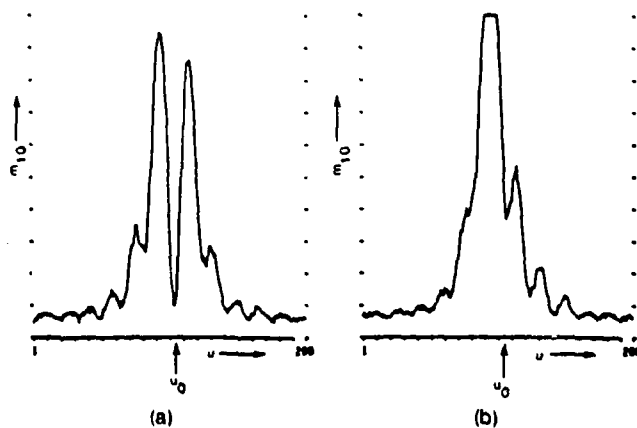


Fig. 5. (a) Line scan through the  $m_{10}$  moment of a binary square with  $x$  symmetry. (b) Line scan through the  $m_{10}$  moment of a binary square shifted in the  $x$  direction with respect to its position in (a).

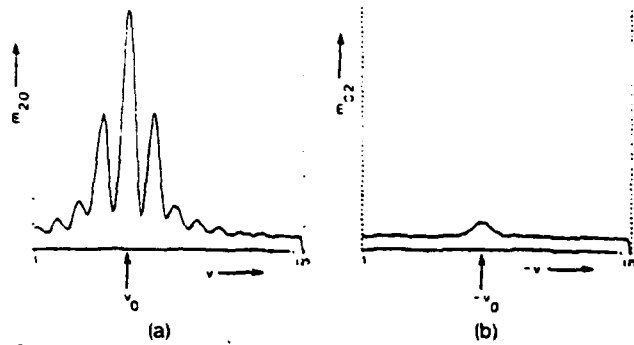


Fig. 6. Line scans through two geometric moments of a rectangle with 2:1 aspect ratio: (a)  $m_{20}$ , (b)  $m_{02}$ .

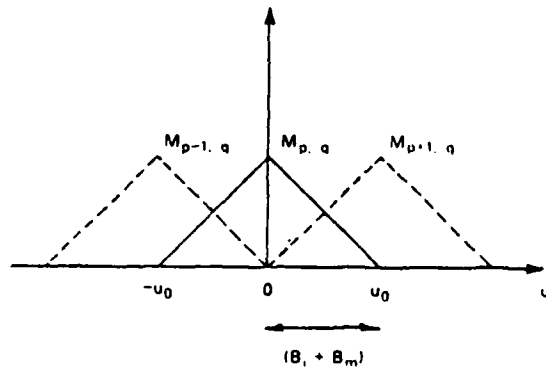


Fig. 7. Distribution in the output plane when  $u_0 = B_i + B_m$ , leading to zero cross talk between adjacent moments.

The use of generating functions other than  $x^m y^n$  could offer significant advantages. For given classes of functions, certain combinations of geometric moments can be determined to be optimum for minimizing intraclass spread while maximizing interclass separation by using standard algorithms.<sup>7</sup> These combinations can then be encoded directly in the computer-generated holographic mask, thus enabling the coherent optical processor to carry out classification of statistical patterns. To extract complex-value moments in the output, the four quadrature components could be treated independently and measured as positive real numbers.

The maximum number of moments that can be calculated in parallel is determined by the single-sided bandwidth of the system (including the computer-generated hologram)  $B_s$ , the single-sided bandwidth of the input function  $B_i$ , and the single-sided bandwidth of the generating function  $B_m$ . Since the output contains a convolution between the Fourier transform of the input and the Fourier transform of the generating function, each term will be extended over a region  $2(B_i + B_m)$  in the frequency plane. The spacing of the moments (determined by  $u_0$  in  $u$  direction and by  $v_0$  in  $v$  direction) should be such that at points  $(mu_0, nv_0)$  only the  $G_{mn}$  will be nonzero; i.e.,  $u_0 = v_0 = (B_i + B_m)$ , as is shown in Fig. 7 for one dimension. Therefore the total number of moments that can be calculated in parallel is given by

$$N = \left[ 2 \left( \frac{B_s}{B_i + B_m} \right) - 1 \right]^2. \quad (5)$$

This number can be increased substantially by using spectrum-shaping techniques on the input; these techniques will be discussed in a subsequent publication.

We would like to thank James Leger of the University of California, San Diego, for providing a copy of the code for generating the computer-generated holograms and Marilyn Blodgett for implementing this code on the Naval Research Laboratory's computer-film-writer system.

\* Permanent address, Department of Electrical Engineering and Computer Sciences, Clarkson College of Technology, Potsdam, New York 13676.

## References

1. M. K. Hu, IEEE Trans. Inf. Theory IT-8, 179 (1962).
2. S. Dudani, K. Breeding, and R. McGhee, IEEE Trans. Comput. C-26, 39 (1977).
3. S. S. Reddi, IEEE Trans. Pattern Anal. Machine Intell. PAMI-3, 240 (1981).
4. M. R. Teague, Appl. Opt. 19, 1353 (1980).
5. D. Casasent and D. Psaltis, Opt. Lett. 5, 395 (1980).
6. W. H. Lee, *Computer-Generated Holograms: Technique and Applications*, Vol. XVI in *Progress in Optics*, E. Wolf, ed. (North-Holland, Amsterdam, 1978).
7. K. Fukunaga, *Introduction to Statistical Pattern Recognition* (Academic, New York, 1972).

# RAPID COMMUNICATIONS

This section was established to reduce the lead time for the publication of Letters containing new, significant material in rapidly advancing areas of optics judged compelling in their timeliness. The author of such a Letter should have his manuscript reviewed by an OSA Fellow who has similar technical interests and is not a member of the author's institution. The Letter should then be submitted to the Editor, accompanied by a LETTER OF ENDORSE-

MENT FROM THE OSA FELLOW (who in effect has served as the referee and whose sponsorship will be indicated in the published Letter). A COMMITMENT FROM THE AUTHOR'S INSTITUTION TO PAY THE PUBLICATION CHARGES, and the signed COPYRIGHT TRANSFER AGREEMENT. The Letter will be published without further refereeing. The latest Directory of OSA Members, including Fellows, is published in the May/June 1982 issue of Optics News.

## Optical matrix-matrix multiplier based on outer product decomposition

Ravindra A. Athale and William C. Collins

U.S. Naval Research Laboratory, Washington, D.C. 20375.

Received 5 March 1982.

Sponsored by Joseph W. Goodman, Stanford University.

Optical processors for multiplying two matrices have been described in the literature.<sup>1-4</sup> Considerable work has been reported recently on performing vector-matrix multiplications with incoherent optical processors.<sup>5,6</sup> It is suggested that matrix-matrix multiplications can be implemented with these processors by inputting one matrix a row at a time while the second matrix is encoded on a 2-D mask. The output matrix is then available one row at a time. All these schemes have one drawback in that they require at least one of the input matrices on a 2-D mask, thus making it difficult to update that matrix at high frame rates with currently available 2-D spatial light modulators (SLM). An optical processor based on a systolic architecture was recently proposed to overcome this drawback.<sup>7</sup> But such a processor requires  $2N - 1$  parallel channels to handle  $N \times N$  matrices and takes  $4N$  clock cycles to perform one vector-matrix multiplication. Thus it does not fully utilize the parallel processing capabilities of optical systems.

These processors are all based on performing the inner product between two vectors for generating one element of the output vector (or matrix). Thus they use dimensionality-reducing operations (from  $N$  to 1). An alternate approach would involve dimensionality-increasing operations such as an outer product between two vectors (from  $N$  to  $N^2$ ). Proposals have been made to use the outer product between two vectors to generate the covariance matrix of those vectors.<sup>8,9</sup> In this Letter we describe the application of the outer product operations to matrix-matrix multiplication.

The matrix multiplication between two  $N \times N$  matrices  $A$  and  $B$  can be stated as follows<sup>10</sup>:

$$C = AB \quad (1)$$

where

$$C_{ij} = \sum_{k=1}^N A_{ik} B_{kj}.$$

Thus the  $ij$ th element of  $C$  is given by the inner product between the  $i$ th row vector of  $A$  and the  $j$ th column vector of  $B$ . Alternatively the output matrix  $C$  can be expressed as a sum of  $N$  matrices:

$$C = \sum_{i=1}^N C^i \quad (2)$$

where

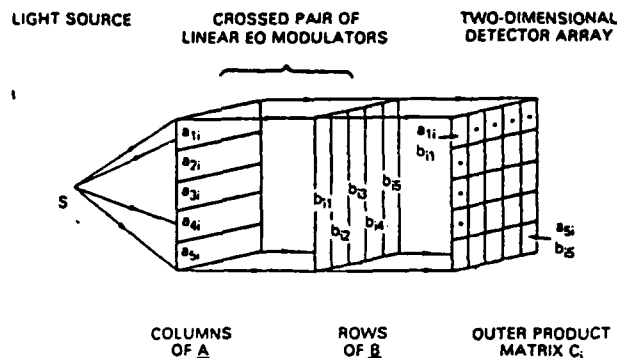


Fig. 1. Schematic diagram of an EO-EO processor for matrix multiplication. The crossed pair of linear modulators and detector plane are shown separated for the sake of clarity.

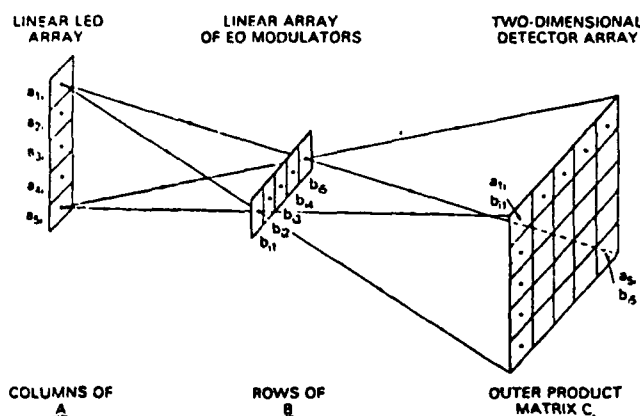


Fig. 2. Schematic diagram of a LED-EO processor for matrix multiplication. Imaging and focusing optics are omitted.

$$C^i = \begin{pmatrix} a_{1i}b_{i1} & a_{1i}b_{i2} & \dots & a_{1i}b_{in} \\ a_{2i}b_{i1} & a_{2i}b_{i2} & \dots & a_{2i}b_{in} \\ \vdots & \vdots & \ddots & \vdots \\ a_{ni}b_{i1} & a_{ni}b_{i2} & \dots & a_{ni}b_{in} \end{pmatrix}.$$

Here each matrix term  $C^i$  in the summation is seen to correspond to an outer product between the  $i$ th column vector of  $A$  and  $i$ th row vector of  $B$ . The outer product between two vectors can be performed optically by crossing two linear-array light modulators as described in Ref. 8. The summation of the different matrix terms in Eq. (2) can be performed in a 2-D integrating detector array. To perform the operation of matrix multiplication between two  $N \times N$  matrices  $A$  and  $B$ ,

the columns of A and rows of B are applied sequentially to the appropriate elements of the crossed pair of linear arrays of light modulators. The light transmitted through the crossed light modulators contains the outer product between two vectors which is detected and summed in a 2-D detector array. Thus it takes  $N$  clock cycles to carry out the matrix multiplication which involves  $N^3$  multiplies and  $N^3$  additions. The optical processor, therefore, performs  $N^2$  multiplies and  $N^2$  additions in parallel. In this algorithm both of the input matrices are required one column (row) vector at a time, and the well-developed technology of 1-D light modulators can be utilized in building the desired optical processor.

The various implementations of this optical processor can use one of the following modulation mechanisms for the linear array of light modulators: electrooptic (EO) modulations, direct driven LED array, or, acoustooptic (AO) Bragg cells.

In this Letter we describe three implementations:

(1) Encoding of both A and B via EO modulators (EO-EO processor) leads to a very compact optical system which does not require any imaging or focusing components such as lenses or fibers. The schematic diagram of the optical processor is shown in Fig. 1, where the two crossed light modulator arrays and detector are shown separated for the sake of clarity. The EO modulators can be constructed out of PLZT electrooptic ceramics which possess good switching speed and require moderate voltages.<sup>11</sup>

(2) The schematic diagram of the optical processor where A is encoded via direct modulation of a LED array and B is encoded via EO modulators (LED-EO processor) is shown in Fig. 2. Here an optical system spreads the LED array output in the horizontal direction while focusing in the vertical direction. The linear array of EO modulators can consist of point modulators instead of the elongated finger modulators required by the EO-EO scheme. The emerging light is then imaged in both horizontal and vertical directions on a 2-D detector array.

(3) The optical processor based on encoding both A and B via Bragg cells (AO-AO processor) is similar to the crossed Bragg cell processors described in the literature for generating Woodward's ambiguity functions<sup>12</sup> (see Fig. 3). The difference in this case is that the light source is pulsed so as to freeze

the acoustic wave in the Bragg cell in time. The columns of A and rows of B modulate an rf carrier which drives the appropriate Bragg cells. When all the elements of the column (row) vector are loaded in the Bragg cell, the light source is pulsed and the outer product is stored in the detector array.

The choice of a particular implementation of the processor will be guided by the format of input matrices as well as the constraints imposed by the volume and power consumption requirements of specific applications.

The overall performance of this optical processor will be determined by the operating characteristics of the light source, the light modulators, and the 2-D detector array. Since the technologies pertaining to the light sources and 1-D modulators are well-developed, the limitation on the accuracy and throughput rate of the processor will be imposed by the 2-D detector array. The main choices for the detector array are going to be CCD array, photodiode array, and vidicon TV camera. As a representative example, if one considers the third implementation of the optical processors (AO-AO) with the vidicon TV camera as the detector, it is possible to multiply two positive  $1000 \times 1000$  matrices in 30 msec corresponding to  $3 \times 10^{10}$  multiplies and  $3 \times 10^{10}$  adds/sec with 8-bit accuracy. Such a matrix-matrix multiplier would be useful in 2-D mathematical transforms, matrix inversion problems, and pattern recognition among other tasks.

Stimulating discussions with D. Stillwell, J. N. Lee, and A. D. Fisher are gratefully acknowledged.

## References

1. R. A. Heinz, J. O. Artman, and S. H. Lee, *Appl. Opt.* 9, 2161 (1970).
2. W. Schneider and W. Fink, *Opt. Acta* 22, 879 (1975).
3. P. N. Tamura and J. C. Wyant, *Proc. Soc. Photo-Opt. Instrum. Eng.* 83, 97 (1976).
4. A. R. Dias, "Incoherent Optical Matrix-Matrix Multiplier," *Optical Information Processing for Aerospace Applications*, NASA Conference Publication 2207 (NTIS, Springfield, Va., 1981).
5. M. A. Monahan, K. Bromley, and R. P. Bocker, *Proc. IEEE* 65, 121 (1977).
6. J. W. Goodman, A. R. Dias, and L. M. Woody, *Opt. Lett.* 2, 1 (1978).
7. H. J. Caulfield et al., *Opt. Commun.* 40, 86 (1981).
8. A. Tarrasevich, N. Zepkin, and W. T. Rhodes, "Matrix Vector Multiplier with Time-Varying Single Dimensional Spatial Light Modulators," *Optical Information Processing for Aerospace Applications*, NASA Conference Publication 2207 (NTIS, Springfield, Va., 1981).
9. J. M. Speiser and H. J. Whitehouse, *Proc. Soc. Photo-Opt. Instrum. Eng.* 293, 41 (1981).
10. For the sake of convenience we will deal with square matrices, although extension to nonsquare matrices will be straightforward.
11. K. Ueno and T. Saku, *Appl. Opt.* 19, 164 (1980).
12. J. D. Cohen, "Ambiguity Processor Architecture Using One-Dimensional Acousto-Optic Transducers," in *Proc. Soc. Photo-Opt. Instrum. Eng.* 180, 134 (1979).

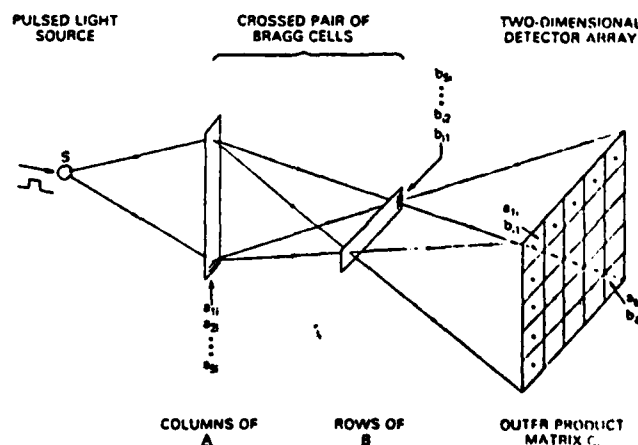


Fig. 3. Schematic diagram of an AO-AO processor for matrix multiplication. Imaging optics as well as spatial filtering are omitted.

# Optical implementation of integral transforms with Bessel function kernels

R. A. Athale, H. H. Szu, and J. N. Lee

Naval Research Laboratory, Washington, D.C. 20375

Received November 12, 1981

Integral transforms involving Bessel function kernels are useful in analyzing effects of circularly symmetric optical systems on arbitrary inputs. Methods for performing the integral transforms optically are divided into two categories. The first category involves input data available in cartesian  $(x, y)$  format and uses the close connection between the desired integral transform and the two-dimensional Fourier transform in cartesian coordinates. The second category involves input data in polar  $(r, \theta)$  format and uses methods such as change of variables to perform the integral transform as a correlation integral. Experimental results obtained with optical implementation for these two categories are presented.

The analysis of complex optical systems is greatly facilitated by two-dimensional Fourier transform techniques. The effect of an optical system on arbitrary inputs is easily described by a transfer function in the Fourier domain. Integral transforms involving Bessel functions are similarly useful when dealing with circularly symmetric (or axisymmetric) systems for arbitrary inputs.<sup>1</sup> This problem is encountered in the mode analysis on the output of a slightly misaligned laser resonator<sup>2,3</sup> or in the alignment of space telescopes. An optical method for performing mode analysis via integral transforms will have the unique advantage of preserving the phase of the wave front to be analyzed, in contrast to the more usual methods involving measurement of the intensity of the wave front.

It is well known that when a two-dimensional function has circular symmetry, its Fourier transform is also circularly symmetric. It can be shown that in such a case the Fourier transform is equivalent to the Hankel transform of the input, which is defined as

$$F_0(\rho) = \int_0^\infty f(r) J_0(\rho r) r dr, \quad (1)$$

where  $J_0(\rho r)$  is the zeroth-order Bessel function.<sup>4</sup> Thus in dealing with circularly symmetric systems, the Hankel transform (which is a one-dimensional integral) can be used instead of the two-dimensional Fourier transform if the inputs are also circularly symmetric. This technique can be extended to functions of the form  $f(r) \exp(jn\theta)$  ( $n$ -fold symmetric) by using the Hankel transform of order  $n$  defined as

$$F_n(\rho) = \int_0^\infty f(r) J_n(\rho r) r dr, \quad (2a)$$

where  $J_n(\rho r)$  is the  $n$ th-order Bessel function. In this case the two-dimensional Fourier transform with respect to  $(x, y)$ —indicated by  $FT_2$ —is related to  $F_n(\rho)$  by<sup>1</sup>

$$FT_2[f(r) \exp(jn\theta)] = 2\pi F_n(\rho) \exp(-jn\phi), \quad (2b)$$

where  $(\rho, \phi)$  are polar variables in the Fourier plane.

The generalized Hankel transform,  $F_{nn}(\rho)$ , can be defined for an arbitrary function  $f(r, \theta)$  as follows<sup>1</sup>:

$$f(r, \theta) = \sum_{n=-\infty}^{\infty} f_n(r) \exp(jn\theta), \quad (3a)$$

$$F_{nn}(\rho) = \int_0^\infty f_n(r) J_n(\rho r) r dr. \quad (3b)$$

The generalized Hankel transform thus involves a Fourier series expansion of  $f(r, \theta)$  with respect to  $\theta$ , followed by the operation of the Hankel transform of order  $n$  on  $f_n(r)$ . In the following we will describe techniques and experimental results for optical implementation of the generalized Hankel transforms. These various techniques are each applicable in different circumstances.

In optical processors a two-dimensional Fourier transform with respect to the cartesian coordinates  $(x, y)$  is performed very easily with the help of a simple spherical lens.<sup>4</sup> The equivalence of the two-dimensional Fourier transform and the Hankel transform for circularly symmetric functions was noted above. For arbitrary functions,  $f(x, y)$ , the following relation exists:

$$FT_2[f(x, y)] = \mathcal{F}(\rho, \phi) = 2\pi \sum_{n=-\infty}^{\infty} F_{nn}(\rho) \exp(-jn\phi), \quad (4)$$

where  $\mathcal{F}(\rho, \phi)$  is the two-dimensional Fourier transform of the input in terms of the polar coordinates  $(\rho, \phi)$ . The generalized Hankel coefficients  $F_{nn}(\rho)$  can thus be extracted by performing a one-dimensional Fourier transform on  $\mathcal{F}(\rho, \phi)$  with respect to  $\phi$ .

$$F_{nn}(\rho) = \int_{-\pi}^{\pi} \mathcal{F}(\rho, \phi) \exp(jn\phi) d\phi. \quad (5)$$

Therefore, a spherical lens first performs the two-dimensional Fourier transform with respect to the cartesian coordinates on the input. A suitably designed computer-generated hologram then performs the coordinate transformation (cartesian to polar) on the Fourier transform, generating  $\mathcal{F}(\rho, \phi)$ .<sup>5</sup> This is followed

ENCLOSURE (3)

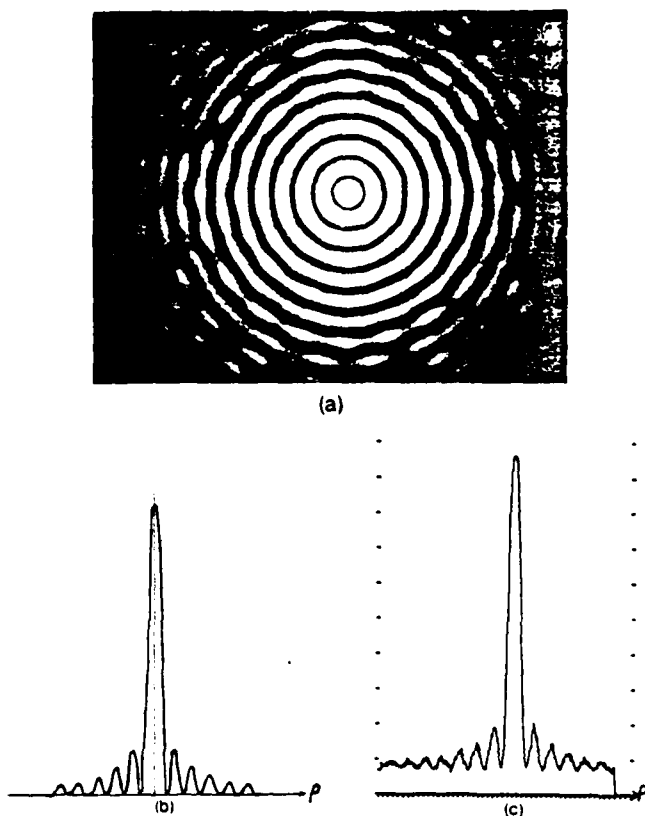


Fig. 1. Experimental results for zeroth-order Hankel transform,  $F_0(\rho)$ , of  $\delta(r - a)$ . (a) Photograph of the output. (b) A plot of  $|J_0(a\rho)|^2$ , which is the theoretically expected result. (c) A line scan through the origin of the pattern in (a), giving  $|F_0(\rho)|^2$  versus  $\rho$ .

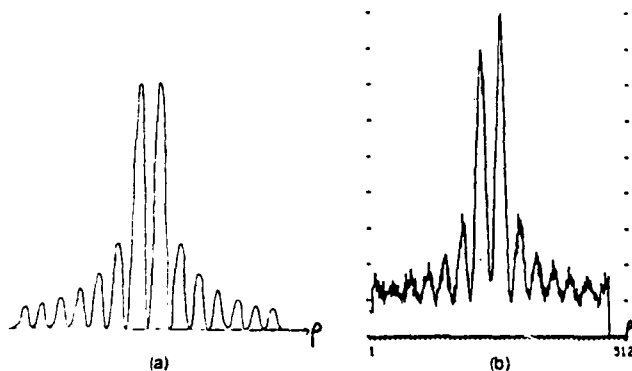


Fig. 2. Experimental results for first-order Hankel transform,  $F_1(\rho)$ , of  $\delta(r - a)$ . (a) A plot of  $|J_1(a\rho)|^2$  versus  $\rho$ , which is the theoretically expected result. (b) A line scan through the origin of the two-dimensional Fourier transform, giving  $|F_1(\rho)|^2$  versus  $\rho$ .

by a cylindrical lens to implement the one-dimensional Fourier transform with respect to  $\phi$ .

Initial optical experiments established the connection between a two-dimensional Fourier transform with respect to cartesian coordinates and a Hankel transform of order  $n$  for a function of the form  $f(r) \exp(jn\theta)$  [Eq. (2b)]. The optical system used was a standard two-dimensional Fourier-transform arrangement.<sup>4</sup> A computer-generated hologram was used to encode a

$\exp(jn\theta)$  dependence onto the input. The output was detected by a TV camera, which measures the light intensity in the Fourier plane of the input. The input used in these experiments had an  $r$  dependence given by  $\delta(r - a)$ , thus corresponding to a thin ring of radius  $a$  in the cartesian  $(x, y)$  plane. The  $n$ th-order Hankel transform of  $\delta(r - a)$  is a  $J_n(a\rho)$ , thus allowing easy comparison with experiments. Figure 1 shows the results corresponding to the Hankel transform [i.e.,  $n = 0$  and  $\exp(jn\theta) = 1$ ]. In Fig. 1(b) the function  $|J_0(a\rho)|^2$  is plotted, which is then compared with a line scan through the origin [Fig. 1(c)] of the output shown in Fig. 1(a), i.e.,  $\phi = 0$ . Very good qualitative agreement between the theoretical and experimental results is obtained. Figures 2(a) and 2(b) present the results for the Hankel transform of order one for the same  $f(r)$ , i.e.,  $\delta(r - a)$  [but here the  $\theta$  dependence is  $\exp(j\theta)$ ]. Again good qualitative agreement was seen between theory and experiment. This system also performed the Hankel transform of order two on the same input with good results.<sup>6</sup>

If the input is polar  $(r, \theta)$  formatted, the direct approach given in Eq. (3) has to be followed in obtaining the generalized Hankel transform. The first part of the operation, which involves a Fourier series expansion in variable  $\theta$ , requires the  $r$  and  $\theta$  coordinates be mapped along orthogonal axes. Then Eq. 3(a) is performed optically using a cylindrical lens. The calculation of the Hankel transform of order  $n$  of  $f_n(r)$ , the  $n$ th coefficient of expansion, is less straightforward, since it involves optically performing a space-variant operation; hence, this was the main aim here.

One way of converting a space-variant operation into a shift-invariant operation is to employ appropriate change of variables. In the case of the Hankel transforms of order  $n$ , the following procedure was described by Siegman for implementing the space-variant operation as a correlation integral on a digital processor.<sup>7</sup> From the definition (2a) one obtains

$$\hat{F}_n(y) = \int_{-\infty}^{\infty} f(x) J_n(x + y) dx, \quad (6)$$

where  $r = r_0 \exp(\alpha x)$ ,  $\rho = \rho_0 \exp(\alpha y)$ ,  $\hat{F}_n(y) = \rho F_n(\rho)$ ,  $f(x) = r f(r)$ ,  $J_n(x + y) = \alpha \rho J_n(r \rho)$ . The algorithm, therefore, consists of first linearly weighting the input  $f(r)$  and performing the  $r \rightarrow x$  coordinates transform. This new input is then correlated with a similarly weighted and coordinate transformed  $n$ th-order Bessel function to give the desired Hankel transform also in linearly weighted and coordinate-distorted form. In any physical system the correlation integral will be performed over a finite interval, giving rise to truncation errors. Also, if the input is sampled in the  $x$  domain, the sampling rate should be adequate to represent the function accurately in the  $x$  domain.<sup>7,8</sup>

Since the operations of coordinate transformation and correlation can be performed by an optical processor, an optical system can be designed and used to calculate  $F_{nn}(\rho)$ . Computer-generated holograms can be used to perform  $r \rightarrow x$  coordinate transformation as well as to encode the Fourier plane filter with impulse response  $J_n(x)$  in a one-dimensional correlator. The second dimension of the optical processor can be used

to perform different-order Hankel transforms on different inputs, thus achieving multichannel operation.

In the experiments, both the input and the Fourier plane filter were encoded by computer-generated holograms. The linear weighting and the coordinate transformation of the input was performed by the digital computer before doing the holographic encoding. The computer-generated holograms used the Lee-Burckhardt technique<sup>9</sup> and contained 128 pixels. The optical system is depicted in Fig. 3. This system was then used to perform the Hankel transform on two different inputs  $f_1(r) = \rho_1 J_0(\rho_1 r)$  and  $f_2(r) = \rho_2 J_0(\rho_2 r)$ . The Hankel transform of  $f_1(r)$  and  $f_2(r)$  should be  $\delta(\rho - \rho_1)$  and  $\delta(\rho - \rho_2)$ , respectively. The results of a computer simulation of this algorithm are depicted in Fig. 4. The finite width of the peak and the appearance of sidelobes are due to the finite limits of integration. To facilitate easy comparison with the experimental results  $|F_0(y)|^2$  was plotted versus  $y$  instead of  $F_0(\rho)$  versus  $\rho$ . Figure 5 shows the experimental results obtained. The optical output was detected by a 1024-element Reticon linear photodiode array. The shift in peak heights (owing to the linear weight) is evident, indicating good qualitative agreement with the computer-simulation results.

This method investigates an approach based on the special properties of Bessel functions. If the input  $f(r)$  is correlated with  $J_m(\rho r)$  then the Hankel coefficient

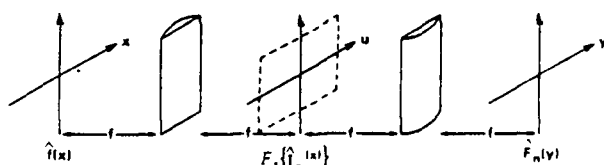


Fig. 3. The schematic diagram of the experimental setup for performing the one-dimensional correlation between the linearly weighted and coordinate-transformed input,  $f(x)$ , and similarly weighted and transformed Bessel function  $J_0(x)$ .

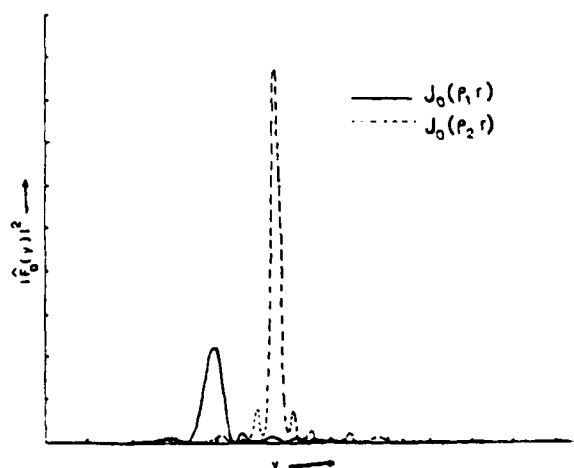


Fig. 4. The results of the computer simulation of zeroth-order Hankel transform of  $\rho_1 J_0(\rho_1 r)$  and  $\rho_2 J_0(\rho_2 r)$ . The linearly weighted and coordinate transformed Hankel coefficients,  $|F_0(y)|^2$ , is plotted versus  $y$ . Here  $\rho_2 = 2\rho_1$ .

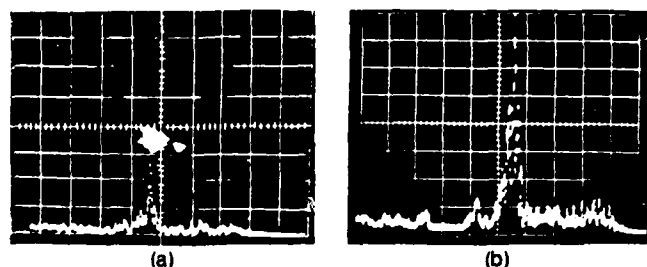


Fig. 5. The oscilloscope traces of the output of the optical processor performing the zeroth-order Hankel transform. The traces correspond to  $|F_0(y)|^2$  versus  $y$  for the two inputs. (a) For input  $f_1(r) = \rho_1 J_0(\rho_1 r)$ . (b) For input  $f_2(r) = \rho_2 J_0(\rho_2 r)$ , where  $\rho_2 = 2\rho_1$ .

of order  $m$ ,  $F_m(\rho)$ , is obtained at the origin of the correlation plane.

$$F_m(\rho) = \int_0^\infty f(r) J_m[\rho(r+r')] r dr |_{r'=0}. \quad (7)$$

The Neumann addition theorem for Bessel functions states that

$$J_m[\rho(r+r')] = \sum_{n=-\infty}^{\infty} J_{m-n}(\rho r') J_n(\rho r). \quad (8)$$

Substituting for  $J_m[\rho(r+r')]$  from Eq. (8) into Eq. (7) we get

$$\begin{aligned} \int_0^\infty f(r) J_m[\rho(r+r')] r dr \\ = \int_0^\infty f(r) \sum_{n=-\infty}^{\infty} J_{m-n}(\rho r') J_n(\rho r) r dr \\ = \sum_{n=-\infty}^{\infty} J_{m-n}(\rho r') F_n(\rho). \end{aligned} \quad (9)$$

Thus, it is seen that the correlation plane contains a sum of Bessel functions of different order weighted by Hankel transform coefficients evaluated at  $\rho$ , of corresponding order. In principle it is possible to extract Hankel transform coefficients of different order out of a single one-dimensional correlation operation. The other dimension of a two-dimensional optical processor can be used to perform correlations with  $J_m(\rho r)$  with different values of  $\rho$ .

## References

1. A. Papoulis, *Systems and Transforms with Applications in Optics* (McGraw-Hill, New York, 1968), Chap. 5.
2. W. H. Southwell, *J. Opt. Soc. Am.* **67**, 396 (1977).
3. C. A. Klein, *Opt. Eng.* **18**, 591 (1979).
4. J. W. Goodman, *An Introduction to Fourier Optics* (McGraw-Hill, New York, 1968), Chap. 2.
5. O. Bryngdahl, *J. Opt. Soc. Am.* **64**, 1092 (1974).
6. R. A. Athale, H. H. Szu, and J. N. Lee, in *Optical Information Processing for Aerospace Applications* (NASA CP-2207, 1981).
7. A. E. Siegman, *Opt. Lett.* **1**, 13 (1977).
8. G. P. Aggarwal and M. Lax, *Opt. Lett.* **6**, 171 (1981).
9. W. H. Lee, "Computer generated holograms: techniques and applications," in *Progress in Optics*, E. Wolf, ed. (North-Holland, Amsterdam, 1978), Vol. XVI.



4-8  
1  
DT